ELSEVIER

Journal of Chromatography A, 878 (2000) 1–15

JOURNAL OF CHROMATOGRAPHY A

www.elsevier.com/locate/chroma

Using a differential refractive index detector as a pressure transducer for online viscometry in exclusion chromatography

Mircea Florea*

ICERP, 291A Republicii Blvd., RO-2000 Ploiesti, Romania

Received 16 February 2000; accepted 18 February 2000

Abstract

A differential refractive index (DRI) detector was tested as a pressure transducer for single capillary online viscometry in exclusion chromatography. The relationship between the detector response and pressure is linear, in agreement with the theoretically expected influence of pressure on refractive index and its dependence on temperature is negligible. Whole polymer and local intrinsic viscosities were determined and compared for narrow and, respectively, broad molecular weight distribution polymer samples. Considering that the detection system described can be improved, the results suggest that modern DRI detectors are susceptible to satisfy the requirements for a suitable pressure transducer in this application.

Keywords: Detection, LC; Refractive index detector; Pressure transducer

1. Introduction

A concentration detector is traditionally used in exclusion chromatography (EC) for providing the weight concentration profile of the polymer elution curve [1,2]. This way is not an absolute method for obtaining molecular weight (M_w) and molecular weight distributions (MD), requiring EC-M_w calibration for each polymer–solvent system. Standards required for conventional calibration are available only for very few polymer materials. The alternative is to determine the polymer M_w in the EC effluent by using M_w-sensitive detectors, such as, light-scattering detectors or viscometer detectors in conjunction with the universal calibration method [3].

In the last decade, on-line viscometer detectors have become commercially available [4,5] and information tremendously increased concerning their assessment and EC-viscometry data reduction. All these detectors are in fact pressure-sensitive detectors, measuring the pressure drop of the eluent passing through capillaries. The pressure drop, ΔP, for laminar flow obeys Poiseuille's equation, being proportional to viscosity, η, which is largely influenced by temperature variations, as well with flow-rate, Q [6,7]:

$$\Delta P = \frac{8}{\pi} L \frac{\eta Q}{\left(\frac{d}{2}\right)^4} \quad (1)$$

where L and d are the length and, respectively, the internal diameter of the capillary.

Several detector designs were described including one to four capillaries in different configurations [8–14], with or without a pulsation damper block or

*Fax: +40-44-199-841.

E-mail address: mflorea@icerp.ro (M. Florea)

0021-9673/00/$ – see front matter
PII: S0021-9673(00)00265-X

using electronic and mathematical filtration methods to remove the interference of flow-rate noise. Temperature variations are eliminated by placing the whole equipment or essential parts of it in a thermostatic compartment.

The differential refractive index (DRI) detector is applicable to many polymers, being the most commonly used concentration detector in EC. However, it shows some drawbacks by comparison with other detectors, as for example, a lower sensitivity to concentration, dependence of refractive index on M_w and an undesirable sensitivity to temperature and pressure. The latest shortcoming is caused by the influence of temperature and pressure on refractive index. For many liquids the variation of refractive index with temperature, $\partial n/\partial T$, is around -4×10^{-4} K^{-1}, while the variation with pressure, $\partial n/\partial P$, is about 5×10^{-5} bar^{-1} [15,16]. To reduce thermal noise, these detectors enclose a large thermal ballast and long inlet tubing to perform necessary heat exchange of the effluent, and, in modern EC dedicated equipment, they are thermostated [17].

Based on the variation of refractive index with pressure, this work demonstrates the use of a DRI detector as a differential pressure transducer for on-line single capillary viscometry in EC. To this purpose, a sufficient sensitivity to pressure is required to allow the use of a capillary with a geometry that ensures good resolution but cause no shear-thinning. The use of capillaries having internal diameters of 0.006″ [11], 0.010″ [12] and 0.014″ [4,7] has been reported. A predictable, simple and stable relationship between detector response and pressure is also required, to permit routine data reduction.

To transform it into a pressure transducer, the DRI detector is used to monitor the variation of refractive index with pressure of the eluent. The two sides of the flow cell are filled with eluent, the outlets of the detector are plugged and the inlets are connected to the ends of the capillary. If the capillary is placed at the end of the chromatographic line, one side of the flow cell is connected to the high-pressure end of the capillary and the other one is left open, at atmospheric pressure. The DRI detector could also function as a differential pressure transducer in a four-capillary bridge configuration [12,13], but this work is limited to experiments with a single capillary. In this way of use of the DRI detector, there is no flow through the detection cell. The influence of the temperature is mostly cancelled, as the detector response is proportional to the difference of refractive indices in the two parts of the flow cell.

First, the relationship between the detector output and pressure was investigated. Then, the merits concerning measuring the pressure drop of EC effluent across a single capillary were evaluated in the case of some narrow MD poly(styrene) (PS) standards and broad PS and poly(methyl methacrylate) (PMMA) samples.

Whole polymer intrinsic viscosities, $[\overline{\eta}]$, can be determined exclusively from the viscometer detector response, independently of the corresponding concentration chromatogram and hence they are not affected by interdetector transport time or differences between cell sizes of the two detectors. Additionally, these are not very sensitive to flow-rate variations and are independent of the resolution of the separation and calibrations. As high shear rates can induce shear-thinning effects, $[\overline{\eta}]$ of polymer samples having high molecular weights was of a special concern. Such phenomena were not yet reported in EC related viscometry, not even in the case of capillaries having I.D. as small as 0.15 mm (0.006″) (shear rate $\sim5\times10^4$ s^{-1}, for a flow-rate of 1 ml/min). However, mechanical shear degradation has been observed in the chromatographic columns for some polymers having M_w higher than 10^6 [18]. Therefore, to check the detector performances and data reduction, $[\overline{\eta}]$ values were determined and compared with dilute solution viscometry results, for high-M_w PS standards. In addition, the Mark Houwink plot obtained from these values was compared with literature data.

Further assessments were done by comparing plots of whole polymer intrinsic viscosities of narrow MD standards with plots of local intrinsic viscosities determined from a broad MD PS sample, versus retention time and molecular weights. Then, using the interdetector transport time derived for PS, an attempt was made to determine the Mark–Houwink constants for a broad PMMA sample.

2. Theory

The variation of refractive index with pressure can be derived by differentiation of one of the well-

known relationships [16,19,20] which express specific refraction, r, as a function of refractive index, n, and density, ρ. They are written in a general form as:

$$f(n) = r\rho \tag{2}$$

differentiation with respect pressure, P, and temperature, T, provides:

$$\mathrm{d}f(n) = \left(\frac{\partial f(n)}{\partial P}\right)_T + \left(\frac{\partial f(n)}{\partial T}\right)_P \tag{3}$$

the term that describes the variation with pressure is written as:

$$\left(\frac{\partial f(n)}{\partial P}\right)_T = r\frac{\partial \rho}{\partial P} + \rho\frac{\partial r}{\partial P} \tag{4}$$

where $\partial r/\partial P$ can be neglected, as r is quasi-independent of pressure (and temperature);

$$\left(\frac{\partial f(n)}{\partial P}\right)_T = \frac{\partial f(n)}{\partial n}\left(\frac{\partial n}{\partial P}\right)_T$$

and

$$\frac{\partial \rho}{\partial P} = \rho\beta,$$

where β represents the isothermal compressibility,

$$\beta = -\frac{1}{V_0}\left(\frac{\partial V}{\partial P}\right)_T$$

with V= volume.

Therefore, the variation with pressure of the refractive index is expressed as:

$$\left(\frac{\partial n}{\partial P}\right)_T = \frac{r\rho\beta}{\dfrac{\partial f(n)}{\partial n}} \tag{5}$$

and substituting $r\rho$ from Eq. (2) gives:

$$\left(\frac{\partial n}{\partial P}\right)_T = g(n)\cdot\beta$$

or for finite but small variations

$$\left(\frac{\Delta n}{\Delta P}\right)_T = g(n)\cdot\beta \tag{6}$$

where

$$g(n) = \frac{1}{\dfrac{\partial \ln(f(n))}{\partial n}}$$

is a constant of which value depends on the form of $f(n)$. For example, in the case of the well known Lorentz–Lorenz equation (e.g., Ref. [16]),

$$f(n) = \frac{n^2-1}{n^2+2}$$

and

$$g(n) = \frac{(n^2-1)(n^2+2)}{6n}.$$

Similarly, the term expressing the variation of refractive index with temperature is expressed as:

$$\left(\frac{\partial n}{\partial T}\right)_P = g(n)\cdot\alpha \quad \text{or} \quad \left(\frac{\Delta n}{\Delta T}\right)_P = g(n)\cdot\beta \tag{7}$$

where α is the thermal dilatation coefficient at constant pressure, and the total variation of the refractive index is given by:

$$\Delta n = g(n)\cdot(\beta\cdot\Delta P + \alpha\cdot\Delta T). \tag{8}$$

The voltage change, ΔE, of the DRI detector is proportional to the difference of refractive indices in the two parts of the flow cell, n_2 and n_1 [21],

$$\Delta E = E - E^* = S\frac{(n_2-n_1)}{n_1} \tag{9}$$

where S/n_1 represents the sensitivity of the DRI detector; E, the detector response; and E^*, the offset of the detector output, equal to the detector response when $n_1 = n_2$.

When used as a differential pressure transducer, the detector output is proportional to the difference of pressures, ΔP, applied on the two sides of the cell:

$$E - E^* = \frac{S\cdot g(n_0)\cdot\beta\cdot(P_2-P_1)}{n_0 + g(n_0)\cdot(\alpha\cdot\Delta T + \beta(P_1-P_0)} \cong k\,\Delta P \tag{10}$$

where n_0 is the refractive index at ambient pressure, P_0; k, a proportionality constant, representing the sensitivity to pressure of the DRI detector, comprising all the previous constants in the above equation

$$(n_0 + g(n_0)\cdot(\alpha\cdot\Delta T + \beta(P_1-P_0) \cong n_0).$$

As it results from Eq. (10) and literature data about the variation of refractive index with temperature [15,16], the influence of the environmental temperature variations on the sensitivity factor, k, is expected to be negligible.

The variation of refractive index with pressure, $(\partial n/\partial P)_T$, determined on the basis of Eq. (10), shows some variation with the form of $f(n)$. Thus, for THF at 20°C and atmospheric pressure, it results 3.8×10^{-5} atm^{-1} with the Gladstone–Dale formula, 4.0×10^{-5} atm^{-1} by using the Eykman formula and 4.3×10^{-5} atm^{-1} for the Lorentz–Lorenz relationship. These values were calculated considering $n=1.40$, and $\beta_0=9.4\times 10^{-5}$ atm^{-1} (informative value supplied by Gilson). No determinations of the refractive index at the wavelength the DRI detector works (950±30 nm) were available; however, it can be estimated from values determined at different wavelengths. The value above was calculated for a wavelength of 950 nm using the Cauchy formula [16] and data at three different wavelengths, $n_\alpha^{20}=1.4051$, $n_\beta^{20}=1.4123$ [22] and $n_D^{20}=1.4072$ [23,26].

3. Experimental

A modular Gilson HPLC system (Gilson Medical Electronics, Middleton, WI, USA) was used to perform EC experiments. This included a 305 pump, a M806 manometric module, a model 116 UV detector tuned at 254 nm for PS or at 230 nm for PMMA and a model 132 DRI detector-connected in series in this order. Alternatively, the above single-piston pump and manometric module were substituted by a Jasco PU-980 two-piston pump (Jasco, Tokyo, Japan). The DRI detector was equipped with a standard analytical (45° angle, 8 μl) flow cell. Data acquisition was performed at a sampling frequency of 10 s^{-1}, through the model 5068 Gilson System Interface Module, by a home-made software, running under MS-Windows. HPLC-grade (LiChroSolv, Merck, Darmstadt, Germany) tetrahydrofuran (THF), passed through an online membrane degasser and a kit of two Zorbax PSM-S bimodal columns (DuPont, Wilmington, DE, USA) were used to perform separation. A Rheodyne 7125 injection valve (Rheodyne, Cotati, CA, USA) with a sample loop of 100 μl was used for sample injection, equipped with a position sensor, which optionally initiates data collection.

To get the detector response versus pressure and viscosity elution curves, the usual flow scheme of the DRI detector has been modified as shown in Fig. 1. The capillary has been connected through a three-way fitting (0.3 mm I.D.) to the inlet of the DRI detector and to the UV detector, respectively. Capillary tubing of different materials and geometry were tested. The results reported in this work were obtained using 0.46 m PEEK tubing of 0.25 mm (0.010″) internal diameter (I.D.). Increasing the flow resistance of the capillary improves the signal-to-noise ratio, but the geometry of the capillary must be a compromise between a low dead volume and a higher I.D., to ensure a good resolution of detection and to avoid shear-thinning effects in the case of higher-M_w macromolecules, respectively. Connections between the column outlet, detectors and capillary were made using tubing of larger I.D. (0.3 mm) to minimise possible flow fluctuations due to the so-called Lesec effect [24,25]. The outlet of the detector channel connected to the capillary was closed tightly, taking care to eliminate air from the tubing. The reference side of the flow cell was filled with eluent and left open.

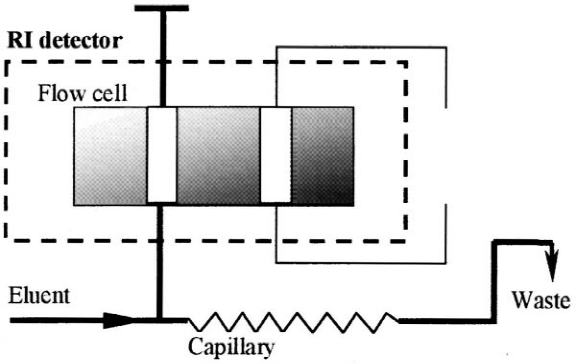

Fig. 1. Flow scheme for using DRI detector as a pressure transducer in a single-capillary configuration.

There are no important restrictions regarding the detector cell endurance. The maximum pressure limit of the DRI detector cell is 0.5 MPa while the UV detector cell withstands up to 3.45 MPa. Employing THF at a flow-rate of 1 ml/min, the pressure drop across the above capillary is 0.036 MPa at 20°C (for a viscosity of THF, $\eta=0.48$ mPa·s [26]). At the same flow-rate and temperature, the shear rate of a Newtonian fluid at the wall of the capillary, e.g. Ref. [27] is 1×10^4 s^{-1} and Reynolds number is 154.

The sensitivity setting of the DRI detector was 6×10^{-6} refractive index units per full scale (ΔRIUFS), which is 5 times higher than when the

detector is used in normal mass detection mode. Else, 'stepped chromatograms' could result, due to the inability of the analog-to-digital converter to distinguish very small voltage changes [28].

The columns, the capillary and the high-pressure filter located before the injector were water-jacketed and maintained at a near ambient temperature with an accuracy of ±0.02°C measured in the thermostat. Good thermal stability of the system was also obtained by keeping the jackets filled with water, without circulation, as it functions as efficient thermal ballast.

Intrinsic viscosities were determined for some samples by dilute solution viscometry at 20°C, using an Ubbelohde glass capillary viscometer in accordance with the ASTM Test Method D445 and following the procedure for in situ dilution described in Ref. [29].

Narrow MD PS standards in the M_w range between 800 and 1 800 000 were supplied by DuPont. A linear calibration relationship (type 1 calibration [30]) was determined using nine PS standards, up to $M_w = 900\,000$: $\log(M_w) = -1.244 \times$ Retention time (min) + 11.035, at a flow-rate of 1.554 ml/min. Toluene was used as flow marker at a concentration of 200 ppm. Concentrations of samples were between 0.05 and 0.1 g/dl. The universal calibration relationship was constructed using literature data on the $[\eta]$ versus M_w relationship for polystyrene [31]. The $\log[\eta]$ versus retention time relationship was limited to the range between 9000 and 900 000, thus obtaining: $\log[\eta] = -0.878 \times$ Retention time (min) + 5.929.

Concentration of samples used in chromatographic determination of intrinsic viscosities were progressively increased from 0.05 g/dl for the highest up to 1 g/dl for the lowest M_w.

An industrial polystyrene sample ($\overline{M}_w = 260\,600$, $\overline{M}_n = 69\,200$, $[\eta] = 89.0$ ml/g) obtained by suspension polymerisation was used to obtain the plot of local intrinsic viscosities versus retention time and molecular weight. A PMMA sample ($\overline{M}_w = 164\,800$, $\overline{M}_n = 68\,100$, $[\eta] = 50.1$ ml/g) was obtained by free radical polymerisation of methyl methacrylate (technical-grade reagent purified by distillation) in toluene, initiated by AIBN at 75°C, followed by several purification steps by dissolution and re-precipitation. These samples were characterised by conventional EC, using the above calibration relationship and literature values of Mark–Houwink constants [31]. In the case of the PS sample MD extends over the calibration range, consequently the values indicated are approximate, affected by extrapolation.

4. Results and discussion

4.1. Detector response versus pressure

With the results derived in the theoretical section, the detector sensitivity to pressure is estimated to be in the range of 630–710 mV atm^{-1}, for a sensitivity setting of 6×10^{-6} Δn per full-scale output of 100 mV. As the sensitivity of DRI depends on the refractive index of the eluent, the value of the sensitivity used could be in error [21].

Experimentally, the DRI detector response to pressure variation was first estimated by applying known static pressures on the detector inlet, by raising and lowering the level of the outlet tubing filled with eluent and observing the voltage change. A linear relationship between voltage change and pressure was observed both when flow was stopped or eluent flowed at a certain constant flow-rate. Taking into account the density of THF to calculate the pressure exerted by the column of liquid, a sensitivity to pressure of about 630 mV atm^{-1} was obtained at an ambient temperature of 24°C, in agreement with the previous theoretical considerations.

Next, the scheme in Fig. 1 was used to monitor the detector response to the pressure drop caused by the flow of the eluent across a capillary. Actual flow-rates were determined by weighing the solvent collected in determined time intervals and taking into account its density at the corresponding temperature.

The relationship between pressure drop across a capillary and both flow-rate and viscosity is linear. However, pressure losses caused by fittings, bending and coiling of the capillary tubing, flow restrictions of diverse nature, entrance and exit of the fluid are independent of viscosity and proportional to the square of the flow-rate, e.g. Ref. [32]. Such pressure losses become as important as the capillary has a lower flow resistance. If such effects are not taken

Fig. 2. Response of DRI detector (used in pressure detection mode) to pressure variations generated by the eluent (THF, at 24°C) flowing across a linear capillary, at different flow-rates.

into account, monitoring the DRI detector signal against flow-rate could erroneously indicate a non-linear variation of the refractive index with pressure.

Fig. 2 illustrates the result of increasing the nominal flow-rate setting, from 0 to 1.5 ml/min by increments of 0.3 ml/min in the case of a linear capillary. The variation of the detector response with flow-rate is very well approximated by a linear relationship, as can be observed in Fig. 3, even if a negligible quadratic term can be identified in the plot of residuals, as in Fig. 4. When the same capillary was used, but it was coiled (radius, 20 mm), the plot of residuals (Fig. 4) shows a significant increase of the quadratic term. It is much more practical to handle a coiled capillary, but because of the observation above this idea was dropped.

The sensitivity to pressure was derived, in the case of the linear capillary, from the slope of the detector signal versus the actual flow-rate divided by the pressure drop. The slope of the detector signal versus flow-rate gives the voltage change for a pressure drop caused by unity flow-rate. The corresponding pressure drop is calculated based on Poiseuille's relationship (Eq. (1)), taking into account the viscosity of THF at the given temperature (data from Ref. [26]). The result is in fair agreement with the value determined by applying static pressure on the detector cell. The exact match of these values is conditioned by the knowledge of the actual bore size of the capillary.

4.2. Pressure elution curves

Fig. 5 contrasts a typical elution curve obtained using the DRI detector as a pressure transducer in single capillary configuration with the concentration elution curve generated by the UV detector. The signal corresponding to the polymer bands decreases with M_w, being also accompanied by a constant and rhythmical flow-rate noise. A slight drift of the base line was almost unavoidable in these experiments, caused by the characteristic thermal drift of the DRI detector response encountered in concentration-detection mode, too, but amplified due to the higher sensitivity setting. The base line drift generally diminished after a longer warm-up period.

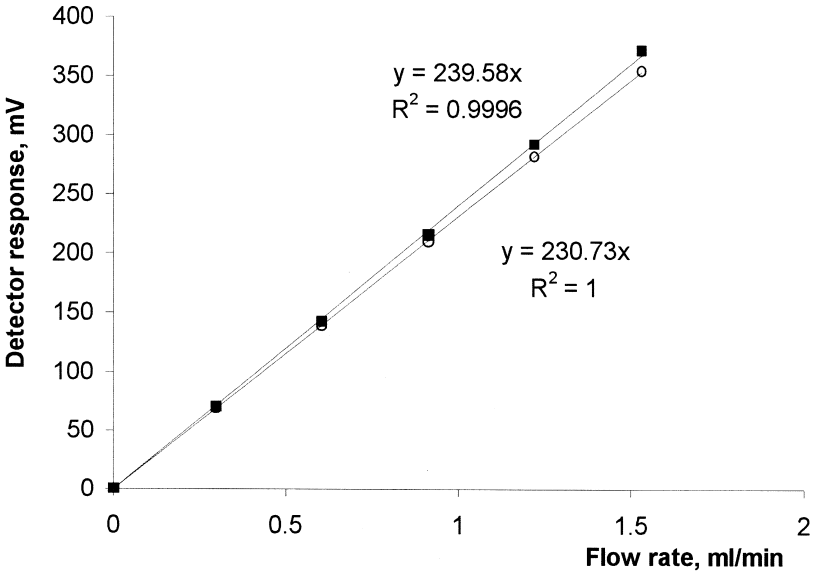

Fig. 3. Detector response versus flow-rate for: (○) linear capillary (data from Fig. 2) and (■) coiled capillary.

Flow fluctuations caused by injection of the sample, and due to the passing of sample from one column into the other, originate a signal variation unnoticed by the concentration detector. These flow fluctuations were more prominent in the case of very high M_w PS standards even for similar specific viscosities. Also, they were larger when the Gilson 305 pump was used along with the 806 manometric module than in the case when these components were substituted by a Jasco PU-980 pump.

Setting the electronic filter incorporated in the DRI detector at a higher time constant produces, besides the smoothing of the elution curve, a significant broadening of the useful signal, too. Numerical

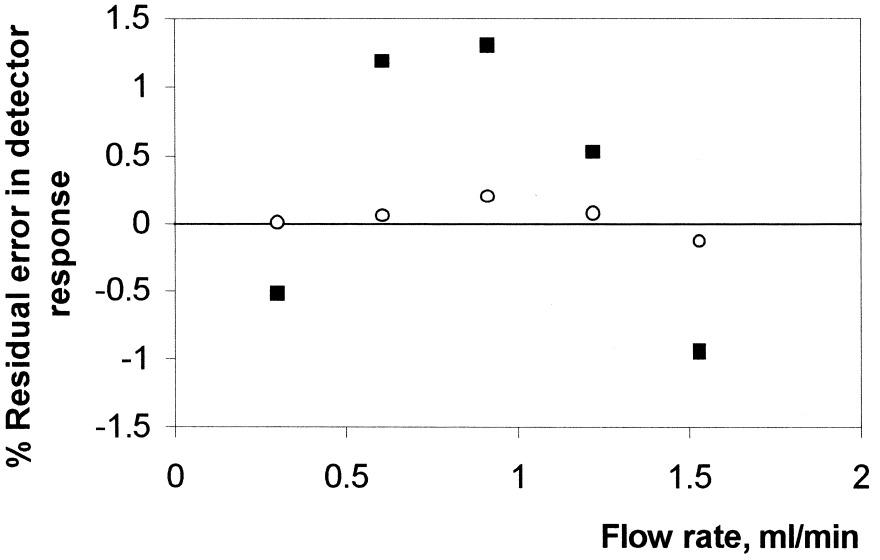

Fig. 4. Plot of residuals for detector response versus flow-rate for Fig. 3: (○) linear capillary and (■) coiled capillary.

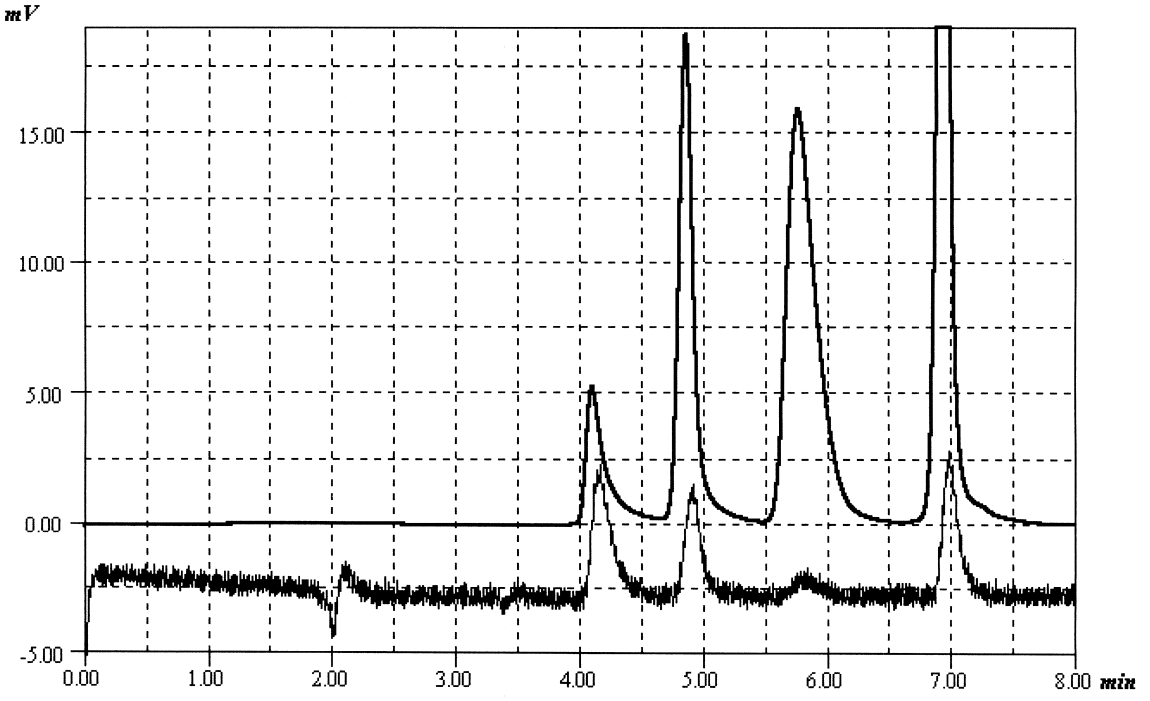

Fig. 5. Typical pressure elution curve as it results from DRI detector in a single capillary configuration (A) and the corresponding UV detector output (B). Pump: Jasco PU-890, nominal flow-rate, 1.5 ml/min. Sample: mixture of polystyrene standards in THF: 900 K, 0.050 g/dl; 109 K, 0.1350 g/dl; 9 K, 0.0226 g/dl; injected volume, 40 μl. Temperature: ambient ~24°C.

filtration methods, such as fast Fourier transform (FFT) [33] and Savitsky–Golay [34] combined with moving average [35,36] provide better smoothing capabilities without significant band broadening, if the corresponding parameters are properly chosen. Good results were also obtained by applying the *ksmooth* function supplied by Mathcad software (Mathsoft), version 7 or higher, which uses a Gaussian kernel to compute local weighted averages of the input vector.

A higher signal-to-noise ratio is expected to be achieved using a higher performance pulse dampener and keeping the DRI detector in a thermostatic environment.

4.3. Intrinsic viscosities

4.3.1. Data reduction

On the basis of Poiseuille's equation and using a simplified Huggins relationship [29], local intrinsic viscosities, $[\eta]_i$, are expressed [4,30] as:

$$[\eta]_i = \frac{1}{c_i}\left[\frac{\Delta P_i - \Delta P_0}{\Delta P_0}\right] \tag{11}$$

where ΔP_0 and ΔP_i are the pressure drops due to the solvent and polymer solution, respectively, and c_i is the local concentration of the polymer solution, corresponding to the ith data point on the pressure elution curve.

By combining Eqs. (10) and (11) and assuming horizontal baseline of the pressure elution curve, local intrinsic viscosities are expressed as:

$$[\eta]_i = \frac{1}{c_i}\frac{E_i - E_0}{E_0 - E^*} \tag{12}$$

where E_i is the ith data point on the chromatogram; E_0, the value of the base line; $E_0 - E^*$, represents the voltage change corresponding to the pressure drop due to the flow of pure eluent, at the respective flow-rate, Q. The ratio $(E_i - E_0)/(E_0 - E^*)$ represents the specific viscosity of the solution, at the corresponding retention time.

Also,

$$c_i = m_i/\Delta V = m_i \cdot f_s/Q, \quad (13)$$

where m_i is the mass of the polymer in the corresponding volume increment, ΔV, and f_s is the sampling frequency. m_i is derived as the product between the total injected mass and the weight fraction of the sample in slice *i*, which is obtained from the corresponding height of the normalised concentration chromatogram.

The bulk (whole sample) intrinsic viscosity, $[\overline{\eta}]$, is given by:

$$[\overline{\eta}] = \frac{\sum_{i=1}^{N} c_i[\eta]_i}{\sum_{i=1}^{N} c_i} \quad (14)$$

where N is the total number of data points in the selected peak region, and

$$[\overline{\eta}] = \frac{\sum_{i=1}^{N}(E_i - E_{0,i})}{(E_0 - E^*) \cdot m \cdot f_s} Q \quad (15)$$

where m is the total injected mass of polymer.

Taking into account second-order terms in Huggins or Kraemer equations proved to be unnecessary in the given experimental conditions. No differences were found between the results provided by the equations above and more sophisticated ones, as cited in Ref. [4].

The detector response to the pressure drop caused by the flow of the eluent, $E_0 - E^*$, is expected to remain constant for constant flow-rate and constant temperature of the capillary. The ratio of the detector response to flow-rate, $(E_0 - E^*)/Q$, in Eq. (15) equals the slope of the detector signal versus flow-rate calibration. Hence, if the temperature of the capillary is kept at the same temperature as the calibration was done, the need for determining the flow-rate in each run is eliminated.

Otherwise, the actual flow-rate, Q, once determined by an absolute method, is monitored and corrected by the use of an internal flow-rate marker [37]. The detector signal, $E_0 - E^*$, can be determined for each run or periodically, for example, by switching off the pump at the end of the chromatogram. Free draining of the eluent must be avoided in this case, since it impairs the result.

Another alternative to find the ratio $(E_0 - E^*)/Q$ is to determine the value that provides the known intrinsic viscosity of a polymer standard.

4.3.2. Whole polymer intrinsic viscosity results

Whole polymer intrinsic viscosities were determined for a series of narrow standards as mean values obtained each from four pressure elution curves and by using Eq. (15). Calculations were preceded by FFT smoothing and base line subtraction. A nominal flow-rate of 1.5 ml/min was used to get a better signal-to-noise ratio. The results are plotted against M_w in Fig. 6, comparatively with a general relationship, of the form:

$$[\eta]_i = K_\Theta \cdot M_i^{1/2} + K' \cdot M_i. \quad (16)$$

This is valid over a wider M_w range and for PS $K_\Theta = 8.512 \pm 0.50 \times 10^{-2}$ ml/g and $K' = 1.742 \pm 0.136 \times 10^{-4}$ ml/g [31]. In the M_w range of 9000–900 000, the experimental $[\overline{\eta}]$ were fitted by a linear relationship which provides Mark–Houwink constants $\alpha = 0.706$ and $K = 0.015$ ml/g. On the basis of these results, it can be concluded that reliable intrinsic viscosities are obtained using the detection method and data reduction described.

In the given conditions shear-thinning effects do not occur up to at least 900 000. The value determined (275 ml/g) for the 1 800 000 sample was much lower than expected (427 ml/g) and than the value obtained by dilute solution viscometry, which was in agreement with literature data. This sample is likely to experience shear degradation by passing through the chromatographic columns.

4.3.3. Local intrinsic viscosity results

Determination of local intrinsic viscosities requires the exact match of concentration and viscosity elution curves. This is unfortunately not easily done by simply correcting for the geometric interdetector volume. In the conditions of EC viscometry, flow fluctuations have been identified by Lesec and coworkers [24,25] that cause viscosity elution curves to be distorted, with an appearance of peak shift toward higher retention times.

The current practice is to determine an interdetector transport time, which allows superimposing intrinsic viscosity versus elution time plots obtained

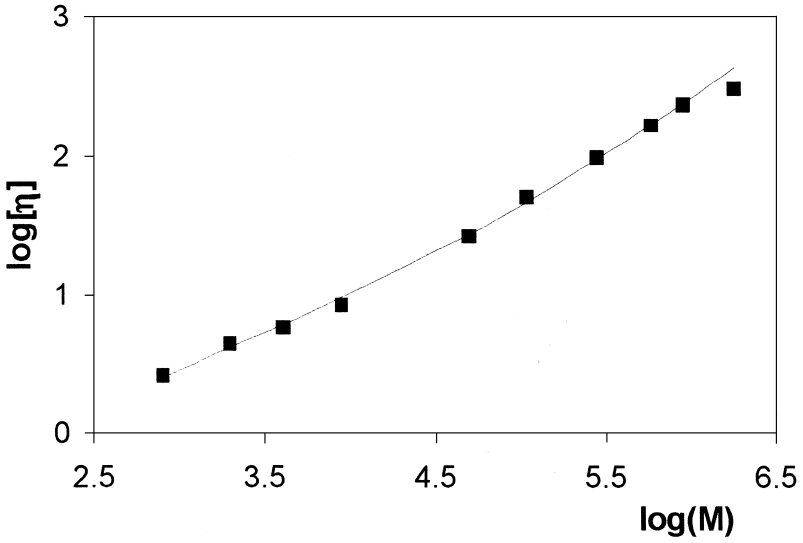

Fig. 6. Plot of intrinsic viscosities of narrow PS standards versus M_w: experimental results (■) in comparison with literature data (—).

from a broad MD standard and, respectively, from a series of narrow MD standards. It has been shown [38] that such an effective interdector volume also makes a correction for axial dispersion.

Peak shifts were evidenced in this study by aligning concentration and viscosity chromatograms of a narrow PS standard to the peaks of a small M_w impurity. It was noticed that the peak of the PS standard on the viscosity curve is abnormally located at a slightly higher elution volume in comparison with the concentration chromatogram. Also, a small broadening of the viscosity chromatograms was observed in comparison to concentration chromatograms. This broadening is likely due to the use of larger I.D. capillaries for connections, which in this case have to be replaced. Other factors that may affect the viscosity chromatograms could be the difference between the volumes of the detector cells, the electronic filter of the DRI detector (the lowest setting of 0.2 s was used), numerical filtration and flow fluctuations.

Under these conditions, determination of $[\eta]_i$ is altered since the specific viscosities and concentrations cannot be exactly fitted. Also, it is expected that the plot $[\eta]_i$ versus retention time derived from chromatograms affected by instrumental dispersion would be lower than the plot of $[\overline{\eta}]$ versus retention time obtained from narrow MD PS samples. Hence, searching for an interdetector volume which allows superimposition of the two plots of $[\eta]$ versus retention time is not rational and further analysis could be worthless, in the given circumstances. Results on determining $[\eta]_i$ from broad MD samples, however, proved to be meaningful with regard to the behaviour of the detection system, especially for the capabilities of the DRI detector as a differential pressure transducer, and consequently are given below.

Viscosity (mean value of three replicates, smoothed by FFT) and concentration chromatograms were determined for the broad PS sample and are presented in Fig. 7. Values of intrinsic viscosities determined by dilute solution viscometry, by conventional EC and by EC with viscometric detection (mean value of three replicates) were in relatively good agreement, 92.7, 89.0 and 88.4 ml/g, respectively.

A weighted least-squares method was applied to find an effective interdetector volume, using as weighting factors the heights of the baseline-subtracted viscosity elution curve, which are proportional to the corresponding specific viscosities. It was considered that in comparison with the errors in determination of specific viscosities, the errors in measurement of concentrations are insignificant. This is justified taking into account the high sensitivity

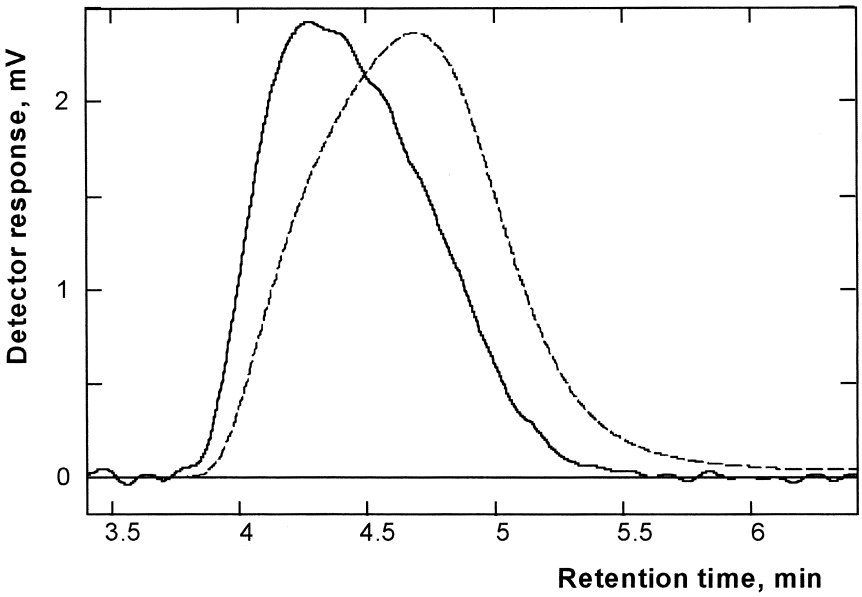

Fig. 7. Concentration (UV 254 nm, - - -) and FFT filtered viscosity (—) chromatograms of broad MD PS sample (concentration, 0.225 g/dl; injected volume, 40 μl; Jasco PU-890 pump, flow-rate, 1.554 ml/min; temperature, ambient).

and stability of the UV detector response in this case. Also, the error in the determination of $\log [\eta]_i$ was considered to be inversely proportional to specific viscosities. This method is similar to that proposed in Ref. [30] with the exception that, in the present work, the errors in determination of concentrations were neglected.

By this method, a value of 109 μl had to be used for the interdetector volume, to superimpose the linear fit of $[\eta]_i$ versus retention time on the plot of $[\overline{\eta}]$ versus retention time derived from narrow standards. The geometrical interdetector volume was estimated to be 25 μl. The fit was restricted to the region between 4 and 5.5 min, discarding that part (3.8–4 min) outside the range of the calibration relationship. This value of the interdetector time appeared to be reproducible at injection volumes of 40, 50 and 60 μl, as well as, at flow-rates of 1.028 and 1.554 ml/min. However, several indications showed that this is too a high value:

- the curvature at the ends of the $[\eta]_i$ versus retention time plot (Fig. 8) and the respective Mark–Houwink plot [39] (Fig. 9), where the corresponding relationships derived from narrow samples are linear
- a trend observed on the plot of residuals, ($\log [\eta]_i$ − linear fit of $\log [\eta]_i$) versus retention time (Fig. 10)
- the comparison of the simulated and experimental viscosity curves (Fig. 11)

Fig. 11 suggests a broadening of the experimental chromatogram, too, and this was also clearly observed on chromatograms obtained at a flow-rate of 1.028 ml/min.

Seeking for an effective interdetector volume failed and this was also confirmed by an attempt made to obtain the Mark–Houwink constants of a broad PMMA sample using the interdetector volume found for PS. Chromatograms and experimental conditions are given in Fig. 12. The Mark–Houwink exponent found was clearly overestimated ($\alpha = 0.79$) and the constant, K, underestimated ($K = 3.8 \times 10^{-3}$ ml/g) and this is attributable to the false interdetector value derived for the PS sample and the lower polydispersity of the PMMA sample. $[\eta]_i$ versus retention time or $[\eta]_i$ versus M_w relationships derived from samples having lower polydispersities show a higher variation with interdetector volume. This suggests that the accuracy of determining Mark–Houwink parameters could be enhanced by

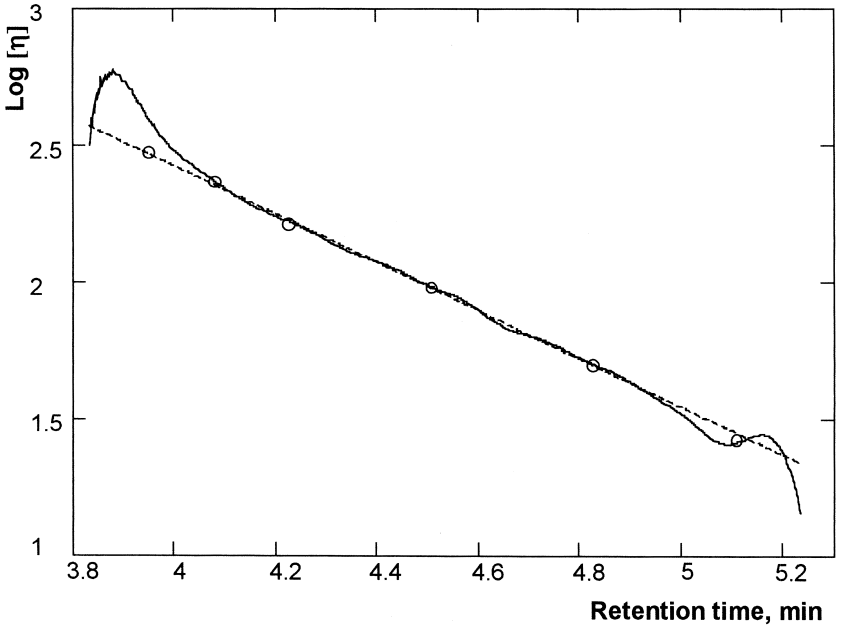

Fig. 8. Local intrinsic viscosities vs. retention time (—), derived from chromatograms in Fig. 7 using an interdetector volume of 109 μl and whole polymer intrinsic viscosities of narrow standards fitted to a linear relationship (– ◦ –).

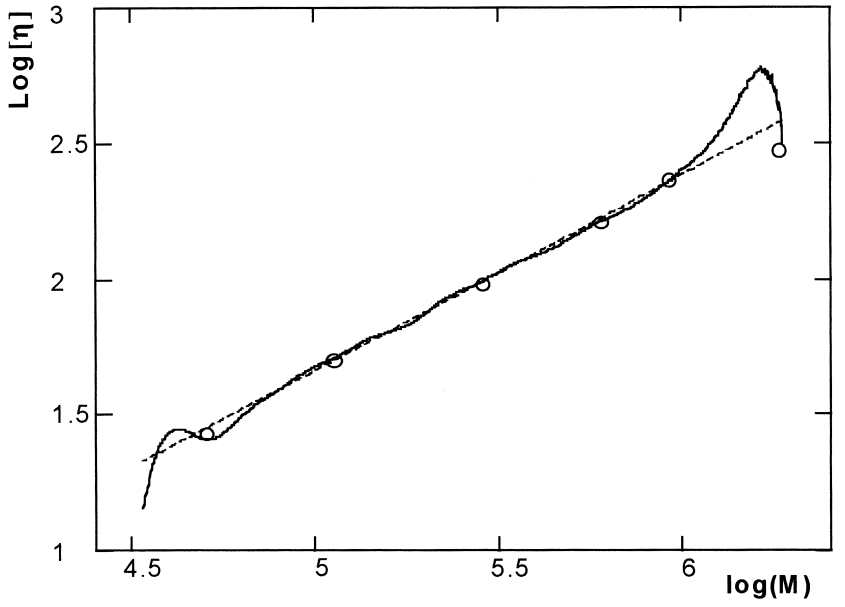

Fig. 9. Mark–Houwink plot derived from chromatograms in Fig. 7 (—) and from narrow MD PS standards (– ◦ –), using an interdetector volume of 109 μl.

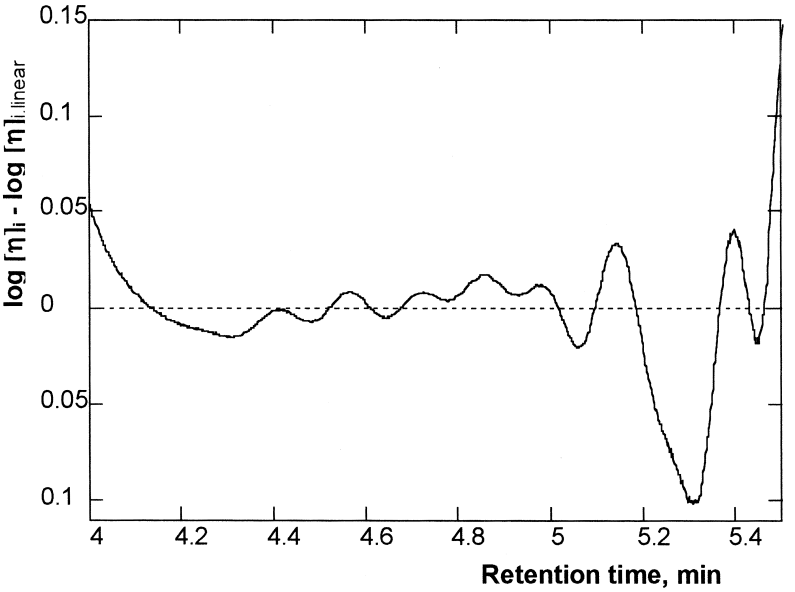

Fig. 10. Plot of residual errors between local intrinsic viscosities versus retention time, as in Fig. 8, and the corresponding regression line.

using an unknown polymer sample having higher polydispersity than the broad PS standard provided that flow fluctuations and axial spreading do not affect differently the corresponding chromatograms.

An interdetector value of 80 μl that minimises the squared differences between $\log [\eta]_i$ and the linear fit of $\log [\eta]_i$ versus retention time for the broad PS sample appears to be a more rational value, in this case. It yields a linear Mark–Houwink plot within the calibration domain, but of course, the values of

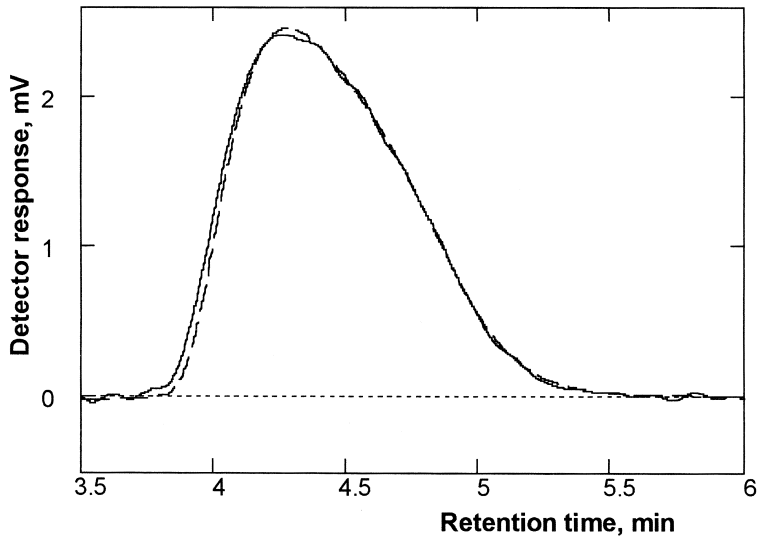

Fig. 11. Experimental (—) and simulated (- - -) viscosity chromatograms corresponding to Fig. 7 and using an interdetector volume of 109 μl.

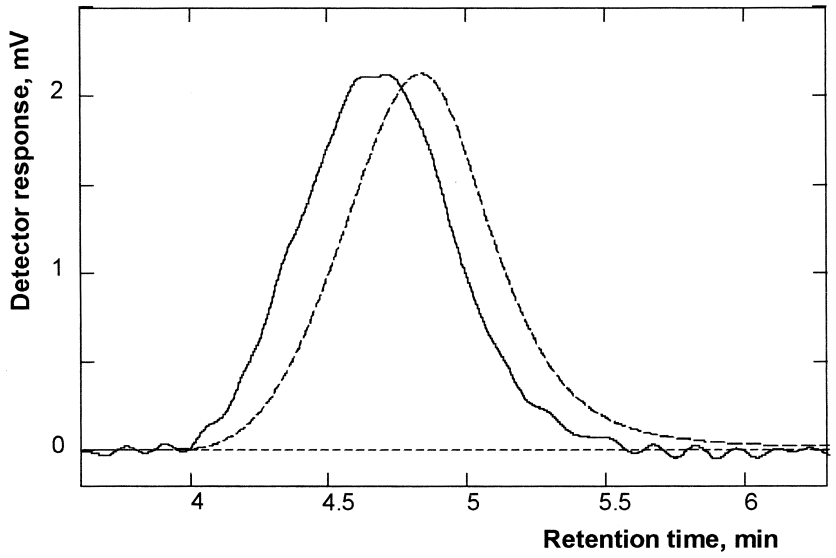

Fig. 12. Concentration (UV 230 nm (- - -)) and FFT filtered viscosity (—) chromatograms of PAMA sample (concentration: 0.312 g/dl, injected volume: 40 μl, Jasco PU-890 pump, flow-rate = 1.554 ml/min, temperature: ambient).

Mark–Houwink parameters are lower than normal for both PS and PMMA, being affected by the broadening of the viscosity chromatogram.

5. Conclusions

A DRI detector was tested as a differential pressure transducer for single capillary online viscometric detection in EC. The relationship between the detector response and pressure is linear, in agreement with the theoretically expected influence of pressure on refractive index. The influence of temperature on the detector sensitivity to pressure is negligible; however, base line drift was almost unavoidable in the normal (not thermostated) working conditions of the detector.

Provided that kinetic and end effects of the capillary can be neglected, the sensitivity factor of the detector is derived from the detector response to the pressure drop caused by the flow of the eluent. Data reduction is as simple as in the case of using an electronic transducer.

Whole polymer and local intrinsic viscosities were determined in order to test the detection system and data processing. Sensitivity to pressure of the DRI detector was high enough to allow the use of a capillary that provides good resolution without shear-thinning effects in the usual M_w and flow-rate ranges.

Determination of accurate interdetector volume, which would allow to obtain reliable Mark–Houwink constants, was not possible, as broadening of the viscosity chromatogram occurred, likely due to higher I.D. connection tubing in the detection area.

Obviously, the detection system described is not yet acceptable for routine analysis, but it is highly susceptible of being improved.

Considering that the design of the detection system and the working conditions of the whole chromatograph can be improved, modern DRI detectors are susceptible to satisfy the requirements for a suitable pressure transducer in this application. Thus, in contrast to the conditions described in this work, one can consider thermostating the whole chromatographic system, using a higher performance pulse dampener, lower I.D. connection tubing in the detection area and perhaps a DRI detector with a lower thermal drift.

References

[1] S.T. Balke, Modern methods of polymer characterization, in: H.G. Barth (Ed.), Chemical Analysis, Vol. 113, Wiley, New York, 1991, p. 1, Ch. 1.
[2] G.R. Meira, Modern methods of polymer characterization, in: H.G. Barth (Ed.), Chemical Analysis, Vol. 113, Wiley, New York, 1991, p. 67, Ch. 2.
[3] Z. Grubisic, P.A. Rempp, H. Benoit, J. Polym. Sci. Part B 5 (1967) 753.
[4] C. Kuo, T. Provder, M.E. Koehler, J. Liq. Chromatogr. 13 (1990) 3177.
[5] W.W. Yau, S.W. Rementer, J. Liq. Chromatogr. 13 (1990) 627.
[6] J. Lesec, M. Millequant, T. Havard, J. Liq. Chromatogr. 17 (1994) 1029.
[7] J.L. Ekmanis, R.A. Skinner, J. Appl. Polym. Sci. Appl. Polym. Symp. 48 (1991) 57.
[8] A.C. Ouano, J. Polym. Sci. Part A-1 10 (1972) 2169.
[9] F.B. Mahili, C. Kuo, M.E. Koehler, T. Provder, A.F. Kah, in: T. Provder (Ed.), Size Exclusion Chromatography, Am. Chem. Soc. Symp. Ser. 245, American Chemical Society, Washington, DC, 1984, p. 281.
[10] W.W. Yau, S.D. Abbot, G.A. Smith, M.Y. Keating, Am. Chem. Soc. Symp. Ser. 352 (1987) 80.
[11] T.A. Chamberlain, H.E. Tuinstra, J. Appl. Polym. Sci. 35 (1998) 1667.
[12] M.A. Haney, J. Appl. Polym. Sci. 30 (1985) 3037.
[13] M.A. Haney, US Patent 4,463,598 (1984).
[14] S. D. Abbot, W. W. Yau, US patent 4,627,271 (1986).
[15] Ullmans Encyklopädie der technischen Chemie, 5 Band, 4th Edition, Verlag Chemie, München, Weinheim, 1980, p. 70
[16] N. Bauer, Technique of organic chemistry, in: A. Weissenberger (Ed.), 2nd Edition, Physical Methods of Organic Chemistry, Part II, Vol. I, Interscience Publishers, New York, 1949, p. 1141.
[17] E. Fotheringham, B.J. Murphy, Int. Lab. 29 (1999) 10.
[18] W.W. Yau, J.J. Kirkland, D.D. Bly, High performance liquid chromatography, in: P.R. Brown, R.A. Hartwick (Eds.), Chemical Analysis, Vol. 98, Wiley, New York, 1989, p. 297, Ch. 6.
[19] I.G. Murgulescu, V.E. Sahini, in: Introducere în Chimia Fizică, Vol. I.2, Editura Academiei, Bucureşti, 1978, p. 359.
[20] B.V. Ioffe, in: Refractometrie Pentru Chimişti, Editura Tehnică, Bucureşti, 1958, p. 12.
[21] P.J. Wyatt, Anal. Chim. Acta 272 (1993) 1.
[22] Landolt – Börnstein, 'Zahlenwerte und Funktionen', II Band, 8 Teil, Springer, Berlin, 1962, p. 645.
[23] L. Scheflan, M.B. Jacobs, in: The Handbook of Solvents, D. van Nostrand, New York, 1953.
[24] J. Lesec, J. Liq. Chromatogr. 17 (1994) 1011.
[25] J. Lesec, M. Milliquant, T. Havard, Polym. Mater. Sci. Eng. 65 (1991) 138.
[26] Ullmans Encyklopädie der technischen Chemie, 17 Band, 3rd Edition, Urban & Scwarzenberg, München, 1966, p. 70
[27] F. Girshick, SAE Paper 929988.
[28] R. Lew, P. Cheung, D. Suwanda, S.T. Balke, J. Appl. Polym. Sci. 35 (1988) 1065.
[29] J.W. Mays, N. Hadjichristidis, Modern methods of polymer characterization, in: H.G. Barth (Ed.), Chemical Analysis, Vol. 113, Wiley, New York, 1991, p. 231.
[30] R. Lew, P. Cheung, S.T. Balke, T.H. Mourey, J. Appl. Polym. Sci. 47 (1993) 1685.
[31] K.G. Suddaby, R.A. Sanayei, K.F. O'Driscoll, A. Rudin, Makromol. Chem. 194 (1993) 1965.
[32] P. Swales, in: M.J. Neale (Ed.), Tribology Handbook, Butterworth, London, 1973, Ch. B25.
[33] R. Shiavi, in: Introduction to Applied Statistical Signal Analysis, Aksen Associates, 1991, p. 68, Ch. 3.
[34] A. Savitzky, M.J.E. Golay, Anal. Chem. 36 (1964) 1627.
[35] F. Baumann, E. Herlicska, A.C. Brown, J. Blesch, in: A. Zlatkis (Ed.), Advances in Chromatography, Marcel Dekker, New York, 1969, p. 263.
[36] F. Schosseler, H. Benoit, Z. Grubisic-Gallot, C. Straziele, Macromolecules 22 (1989) 400.
[37] Th.H. Mourey, S.T. Balke, in: T. Provder (Ed.), Chromatography of Polymers — Characterization by SEC and FFF, Am. Chem. Soc. Symp. Ser, 521, American Chemical Society, Washington, DC, 1993, p. 180, Ch. 12.
[38] P. Cheung, R. Lew, S.T. Balke, T.H. Mourey, J. Appl. Polym. Sci. 47 (1993) 1701.
[39] M. Guaita, O. Chiantore, J. Liq. Chromatogr. 16 (1993) 633.